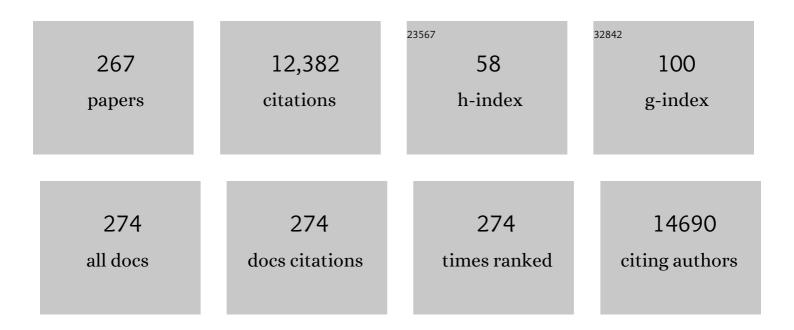
## **Emmanuel Stratakis**

List of Publications by Year in descending order

Source: https://exaly.com/author-pdf/3309571/publications.pdf Version: 2024-02-01



#	Article	IF	CITATIONS
1	Highly sensitive ozone and hydrogen sensors based on perovskite microcrystals directly grown on electrodes. Journal of Materiomics, 2022, 8, 446-453.	5.7	12
2	Strong Eu3+ luminescence in Lа1-x-yErx/2Eux/2CayVO4 nanocrystals: The result of co-doping optimization. Journal of Luminescence, 2022, 242, 118587.	3.1	6
3	Probing the effect of a glass network on the synthesis and luminescence properties of composite perovskite glasses [Invited]. Optical Materials Express, 2022, 12, 823.	3.0	4
4	Advanced composite glasses with metallic, perovskite, and two-dimensional nanocrystals for optoelectronic and photonic applications. Nanoscale, 2022, 14, 2966-2989.	5.6	27
5	How the Physicochemical Properties of Manufactured Nanomaterials Affect Their Performance in Dispersion and Their Applications in Biomedicine: A Review. Nanomaterials, 2022, 12, 552.	4.1	33
6	Ultrashort pulsed laser induced complex surface structures generated by tailoring the melt hydrodynamics. Opto-Electronic Advances, 2022, 5, 210052-210052.	13.3	26
7	Fabrication of Biomimetic 2D Nanostructures through Irradiation of Stainless Steel Surfaces with Double Femtosecond Pulses. Nanomaterials, 2022, 12, 623.	4.1	3
8	Grapheneâ€Enabled Electrophoretic Ion Pump Delivery Devices. Advanced Materials Interfaces, 2022, 9, .	3.7	2
9	Laser-Induced Morphological and Structural Changes of Cesium Lead Bromide Nanocrystals. Nanomaterials, 2022, 12, 703.	4.1	3
10	Fast and selective reduction of nitroarenes under visible light with an earth-abundant plasmonic photocatalyst. Nature Nanotechnology, 2022, 17, 485-492.	31.5	78
11	Nonlinear Optical Imaging of Inâ€Plane Anisotropy in Twoâ€Dimensional SnS. Advanced Optical Materials, 2022, 10, .	7.3	7
12	Charge carrier dynamics in different crystal phases of CH <sub>3</sub> NH <sub>3</sub> PbI <sub>3</sub> perovskite. , 2022, 1, 210005-210005.		6
13	Laser-Induced Erasable and Re-Writable Waveguides within Silver Phosphate Glasses. Materials, 2022, 15, 2983.	2.9	1
14	Optical Simulation Study of Perovskite/CIGS Tandem Solar Cells With Reduced Graphene Oxide Layers. Frontiers in Photonics, 2022, 3, .	2.4	0
15	Nonlinear Optical Imaging of Inâ€Plane Anisotropy in Twoâ€Dimensional SnS (Advanced Optical Materials) Tj ETO	2qJ_1 0.78	84314 rgBT
16	Laser induced periodic surface structures as polarizing optical elements. Applied Surface Science, 2021, 541, 148470.	6.1	24
17	Neuronal Migration on Silicon Microcone Arrays with Different Pitches. Advanced Healthcare Materials, 2021, 10, e2000583.	7.6	5
18	Advanced Photonic Processes for Photovoltaic, Energy Storage, and Environmental Systems. Advanced Sustainable Systems, 2021, 5, 2000237.	5.3	10

#	Article	IF	CITATIONS
19	Three-dimensional characterization of collagen remodeling in cell-seeded collagen scaffolds via polarization second harmonic generation. Biomedical Optics Express, 2021, 12, 1136.	2.9	11
20	Probing valley population imbalance in transition metal dichalcogenides via temperature-dependent second harmonic generation imaging. Npj 2D Materials and Applications, 2021, 5, .	7.9	12
21	Laser Nanostructuring for Diffraction Grating Based Surface Plasmon-Resonance Sensors. Nanomaterials, 2021, 11, 591.	4.1	9
22	Tailoring submicrometer periodic surface structures via ultrashort pulsed direct laser interference patterning. Physical Review B, 2021, 103, .	3.2	35
23	Tuning the valley polarization in WS2 monolayers via control of active defect sites induced by photochemical doping. Applied Physics Letters, 2021, 118, .	3.3	9
24	Dispersion behaviour of two dimensional monochalcogenides. Journal of Colloid and Interface Science, 2021, 594, 334-341.	9.4	4
25	Self-Assembled Dichroic Plasmonic Nitride Nanostructures with Broken Centrosymmetry for Second-Harmonic Generation. ACS Applied Nano Materials, 2021, 4, 8789-8800.	5.0	3
26	Optical versus electron diffraction imaging of Twist-angle in 2D transition metal dichalcogenide bilayers. Npj 2D Materials and Applications, 2021, 5, .	7.9	6
27	Incident angle influence on ripples and grooves produced by femtosecond laser irradiation of silicon. Applied Surface Science, 2021, 570, 151150.	6.1	5
28	Combined effect of shear stress and laser-patterned topography on Schwann cell outgrowth: synergistic or antagonistic?. Biomaterials Science, 2021, 9, 1334-1344.	5.4	7
29	Study of Structure of Defect Centers in Europium Vanadate Nanoparticles with Heterovalent Dopants. , 2021, , .		0
30	Biomonitoring Air Pollution in Carob Leaves. Biology and Life Sciences Forum, 2021, 4, 50.	0.6	1
31	Physiological Characteristics of Expanding and Expanded Leaves of Vitis vinifera L. cv. Assyrtiko in Climate Change Conditions. Biology and Life Sciences Forum, 2021, 4, 55.	0.6	3
32	Polarization-Resolved Second Harmonic Generation for deep 3D characterization of collagen-based scaffold remodeling. , 2021, , .		0
33	Real-time spatially resolved determination of twist angle in transition metal dichalcogenide heterobilayers. 2D Materials, 2021, 8, 015015.	4.4	7
34	Impact of Pre-Patterned Structures on Features of Laser-Induced Periodic Surface Structures. Molecules, 2021, 26, 7330.	3.8	6
35	Thin Films of La1-xSmxVO4:Ca Luminescent Vanadate Nanoparticles Deposited with Various Methods on Glass Substrates. Springer Proceedings in Physics, 2021, , 363-383.	0.2	0
36	Culturing Human Pluripotent Stem Cells on Micropatterned Silicon Surfaces. Methods in Molecular Biology, 2021, , 1.	0.9	0

#	Article	IF	CITATIONS
37	Excitation dependent photoluminescence from quantum confined ultrasmall SnS sheets. Applied Physics Letters, 2021, 119, 241902.	3.3	3
38	Effects of static and dynamic femtosecond laser modifications of Ti/Zr multilayer thin films. European Physical Journal D, 2021, 75, 1.	1.3	4
39	Controlling the wettability of stainless steel from highly-hydrophilic to super-hydrophobic by femtosecond laser-induced ripples and nanospikes. RSC Advances, 2020, 10, 37956-37961.	3.6	37
40	Porous collagen scaffold micro-fabrication: feature-based process planning for computer numerically controlled laser systems. International Journal of Advanced Manufacturing Technology, 2020, 111, 749-763.	3.0	2
41	Biofabrication for neural tissue engineering applications. Materials Today Bio, 2020, 6, 100043.	5.5	82
42	Pulsed laser deposition of the LaVO4:Eu, Ca nanoparticles on glass and silicon substrates. Applied Nanoscience (Switzerland), 2020, 10, 5053-5061.	3.1	1
43	Highly stable metal halide perovskite microcube anodes for lithium-air batteries. Journal of Power Sources Advances, 2020, 3, 100015.	5.1	18
44	Robust B-exciton emission at room temperature in few-layers of MoS2:Ag nanoheterojunctions embedded into a glass matrix. Scientific Reports, 2020, 10, 15697.	3.3	9
45	Molding Wetting by Laser-Induced Nanostructures. Applied Sciences (Switzerland), 2020, 10, 6008.	2.5	4
46	Laser-Assisted Synthesis of Composite Nanoparticles of Perovskite BaTiO3 in Aqueous Solutions and Their Optical Properties. Materials, 2020, 13, 4086.	2.9	2
47	Recent Advances in 2D Metal Monochalcogenides. Advanced Science, 2020, 7, 2001655.	11.2	58
48	Response of NIH 3T3 Fibroblast Cells on Laser-Induced Periodic Surface Structures on a 15×(Ti/Zr)/Si Multilayer System. Nanomaterials, 2020, 10, 2531.	4.1	5
49	Predictive modeling approaches in laser-based material processing. Journal of Applied Physics, 2020, 128, 183102.	2.5	10
50	Highly luminescent and ultrastable cesium lead bromide perovskite patterns generated in phosphate glass matrices. Nanoscale, 2020, 12, 13697-13707.	5.6	26
51	Ionisation processes and laser induced periodic surface structures in dielectrics with mid-infrared femtosecond laser pulses. Scientific Reports, 2020, 10, 8675.	3.3	21
52	Laser engineering of biomimetic surfaces. Materials Science and Engineering Reports, 2020, 141, 100562.	31.8	180
53	Laser-induced topographies enable the spatial patterning of co-cultured peripheral nervous system cells. Materials Science and Engineering C, 2020, 115, 111144.	7.3	9
54	On the formation and features of the supra-wavelength grooves generated during femtosecond laser surface structuring of silicon. Applied Surface Science, 2020, 528, 146607.	6.1	29

#	Article	IF	CITATIONS
55	Neural stem cell delivery via porous collagen scaffolds promotes neuronal differentiation and locomotion recovery in spinal cord injury. Npj Regenerative Medicine, 2020, 5, 12.	5.2	60
56	Effect of a liquid environment on single-pulse generation of laser induced periodic surface structures and nanoparticles. Nanoscale, 2020, 12, 7674-7687.	5.6	34
57	Use of Cotton Textiles Coated by Ir(III) Tetrazole Complexes within Ceramic Silica Nanophases for Photo-Induced Self-Marker and Antibacterial Application. Nanomaterials, 2020, 10, 1020.	4.1	3
58	Modeling ultrafast out-of-equilibrium carrier dynamics and relaxation processes upon irradiation of hexagonal silicon carbide with femtosecond laser pulses. Physical Review B, 2020, 101, .	3.2	13
59	Nanomedicines and Nanosimilars: Looking for a New and Dynamic Regulatory "Astrolabe―Inspired System. AAPS PharmSciTech, 2020, 21, 65.	3.3	4
60	Laser-Assisted Fabrication for Metal Halide Perovskite-2D Nanoconjugates: Control on the Nanocrystal Density and Morphology. Nanomaterials, 2020, 10, 747.	4.1	6
61	Biocompatible polymeric electrospun matrices: Micro–nanotopography effect on cell behavior. Journal of Applied Polymer Science, 2020, 137, 49223.	2.6	16
62	Neuroâ€ŧaxis: Neuronal movement in gradients of chemical and physical environments. Developmental Neurobiology, 2020, 80, 361-377.	3.0	17
63	Prominent room temperature valley polarization in WS2/graphene heterostructures grown by chemical vapor deposition. Applied Physics Letters, 2020, 116, .	3.3	25
64	Omnidirectional iridescence via cylindrically- polarized femtosecond laser processing. Opto-Electronic Advances, 2020, 3, 190035-190035.	13.3	56
65	Nitrogen-Doped Carbon Nanotube/Polypropylene Composites with Negative Seebeck Coefficient. Journal of Composites Science, 2020, 4, 14.	3.0	22
66	Borate-Vanadate Glass-Ceramic Composites Doped with Crystalline Luminescent Oxide Nanoparticles. , 2020, , .		0
67	Deposition of Luminescent Vanadate Nanoparticles on Silicon Solar Cells. , 2020, , .		1
68	Structure and spectroscopy characterization of La1-xSmxVO4 luminescent nanoparticles synthesized co-precipitation and sol-gel methods. Optical Materials, 2019, 95, 109248.	3.6	7
69	Perovskite nanocrystals for energy conversion and storage. Nanophotonics, 2019, 8, 1607-1640.	6.0	78
70	Femtosecond Laser Fabrication of Stable Hydrophilic and Anti-Corrosive Steel Surfaces. Materials, 2019, 12, 3428.	2.9	16
71	<i>In situ</i> monitoring of the charge carrier dynamics of CH <sub>3</sub> NH <sub>3</sub> PbI <sub>3</sub> perovskite crystallization process. Journal of Materials Chemistry C, 2019, 7, 12170-12179.	5.5	10
72	Twist Angle mapping in layered WS2 by Polarization-Resolved Second Harmonic Generation. Scientific Reports, 2019, 9, 14285.	3.3	31

#	Article	IF	CITATIONS
73	All-inorganic lead halide perovskite nanohexagons for high performance air-stable lithium batteries. Nanoscale, 2019, 11, 882-889.	5.6	63
74	Limitations of a polymer-based hole transporting layer for application in planar inverted perovskite solar cells. Nanoscale Advances, 2019, 1, 3107-3118.	4.6	35
75	Biomimetic Omnidirectional Antireflective Glass via Direct Ultrafast Laser Nanostructuring. Advanced Materials, 2019, 31, e1901123.	21.0	103
76	Ligand-free all-inorganic metal halide nanocubes for fast, ultra-sensitive and self-powered ozone sensors. Nanoscale Advances, 2019, 1, 2699-2706.	4.6	44
77	Modelling of the ultrafast dynamics and surface plasmon properties of silicon upon irradiation with mid-IR femtosecond laser pulses. Physical Review B, 2019, 99, .	3.2	25
78	Recent Advances in Femtosecond Laser-Induced Surface Structuring for Oil–Water Separation. Applied Sciences (Switzerland), 2019, 9, 1554.	2.5	41
79	Broad-band high-gain room temperature photodetectors using semiconductor–metal nanofloret hybrids with wide plasmonic response. Nanoscale, 2019, 11, 6368-6376.	5.6	6
80	Laser micro-structured Si scaffold-implantable vaccines against Salmonella Typhimurium. Vaccine, 2019, 37, 2249-2257.	3.8	5
81	The Role of Ligands in the Chemical Synthesis and Applications of Inorganic Nanoparticles. Chemical Reviews, 2019, 119, 4819-4880.	47.7	709
82	Laser-Assisted Surface Texturing of Ti/Zr Multilayers for Mesenchymal Stem Cell Response. Coatings, 2019, 9, 854.	2.6	6
83	Nanoscale Optical Diagnostics of 2D TMDs. , 2019, , .		0
84	Laser-Induced Multi-Functional Biomimetic Surfaces. , 2019, , .		0
85	Spatially selective reversible charge carrier density tuning in WS <sub>2</sub> monolayers via photochlorination. 2D Materials, 2019, 6, 015003.	4.4	13
86	Efficient and environmental-friendly perovskite solar cells via embedding plasmonic nanoparticles: an optical simulation study on realistic device architectures. Optics Express, 2019, 27, 31144.	3.4	28
87	Imaging the crystal orientation of 2D transition metal dichalcogenides using polarization-resolved second-harmonic generation. Opto-Electronic Advances, 2019, 2, 19002601-19002608.	13.3	12
88	Enhancement of the Power-Conversion Efficiency of Organic Solar Cells via Unveiling an Appropriate Rational Design Strategy in Indacenodithiophene-alt-quinoxaline π-Conjugated Polymers. ACS Applied Materials & Interfaces, 2018, 10, 10236-10245.	8.0	11
89	Controlling the Outgrowth and Functions of Neural Stem Cells: The Effect of Surface Topography. ChemPhysChem, 2018, 19, 1143-1163.	2.1	36
90	α,β-Unsubstituted <i>meso</i> -positioning thienyl BODIPY: a promising electron deficient building block for the development of near infrared (NIR) p-type donor–acceptor (D–A) conjugated polymers. Journal of Materials Chemistry C, 2018, 6, 4030-4040.	5.5	22

#	Article	IF	CITATIONS
91	Control of periodic surface structures on silicon by combined temporal and polarization shaping of femtosecond laser pulses. Applied Surface Science, 2018, 444, 154-160.	6.1	31
92	Perovskite nanostructures for photovoltaic and energy storage devices. Journal of Materials Chemistry A, 2018, 6, 9765-9798.	10.3	90
93	Extending the Continuous Operating Lifetime of Perovskite Solar Cells with a Molybdenum Disulfide Hole Extraction Interlayer. Advanced Energy Materials, 2018, 8, 1702287.	19.5	121
94	Formation of periodic surface structures on dielectrics after irradiation with laser beams of spatially variant polarisation: a comparative study. Applied Physics A: Materials Science and Processing, 2018, 124, 1.	2.3	27
95	Investigation of femtosecond laser induced ripple formation on copper for varying incident angle. AIP Advances, 2018, 8, 015212.	1.3	33
96	Laser ablation and injection moulding as techniques for producing micro channels compatible with Small Angle X-Ray Scattering. Microelectronic Engineering, 2018, 195, 7-12.	2.4	4
97	Cells on hierarchically-structured platforms hosting functionalized nanoparticles. Biomaterials Science, 2018, 6, 1469-1479.	5.4	4
98	Modelling periodic structure formation on 100Cr6 steel after irradiation with femtosecond-pulsed laser beams. Applied Physics A: Materials Science and Processing, 2018, 124, 1.	2.3	52
99	Effect of composition and temperature on the second harmonic generation in silver phosphate glasses. Optical Materials, 2018, 75, 796-801.	3.6	9
100	Erasable and rewritable laser-induced gratings on silver phosphate glass. Applied Physics A: Materials Science and Processing, 2018, 124, 1.	2.3	7
101	Biomimetic surface structures in steel fabricated with femtosecond laser pulses: influence of laser rescanning on morphology and wettability. Beilstein Journal of Nanotechnology, 2018, 9, 2802-2812.	2.8	29
102	Novel Biomaterials for Tissue Engineering 2018. International Journal of Molecular Sciences, 2018, 19, 3960.	4.1	20
103	Unveiling the Structure of MoS <i><sub>x</sub></i> Nanocrystals Produced upon Laser Fragmentation of MoS <sub>2</sub> Platelets. ACS Omega, 2018, 3, 16728-16734.	3.5	10
104	Controlling the Wettability of Steel Surfaces Processed with Femtosecond Laser Pulses. ACS Applied Materials & Interfaces, 2018, 10, 36564-36571.	8.0	75
105	Multiscale in modelling and validation for solar photovoltaics. EPJ Photovoltaics, 2018, 9, 10.	1.6	6
106	Improved Charge Carrier Dynamics of CH <sub>3</sub> NH <sub>3</sub> PbI <sub>3</sub> Perovskite Films Synthesized by Means of Laser-Assisted Crystallization. ACS Applied Energy Materials, 2018, 1, 5101-5111.	5.1	31
107	Anion exchange in inorganic perovskite nanocrystal polymer composites. Chemical Science, 2018, 9, 8121-8126.	7.4	24
108	Engineering Cell Adhesion and Orientation via Ultrafast Laser Fabricated Microstructured Substrates. International Journal of Molecular Sciences, 2018, 19, 2053.	4.1	25

#	Article	IF	CITATIONS
109	Ultrahigh-resolution nonlinear optical imaging of the armchair orientation in 2D transition metal dichalcogenides. Light: Science and Applications, 2018, 7, 18005-18005.	16.6	53
110	Laser Nano-Structuring of Pre-Structured Substrates. Journal of Laser Micro Nanoengineering, 2018, 13, 6-9.	0.1	1
111	Improving stability of organic devices: a time/space resolved structural monitoring approach applied to plasmonic photovoltaics. Solar Energy Materials and Solar Cells, 2017, 159, 617-624.	6.2	20
112	Controlling the morphology and outgrowth of nerve and neuroglial cells: The effect of surface topography. Acta Biomaterialia, 2017, 51, 21-52.	8.3	171
113	Efficiency and stability enhancement of inverted perovskite solar cells via the addition of metal nanoparticles in the hole transport layer. RSC Advances, 2017, 7, 12998-13002.	3.6	37
114	Size-Tuning of WSe <sub>2</sub> Flakes for High Efficiency Inverted Organic Solar Cells. ACS Nano, 2017, 11, 3517-3531.	14.6	90
115	Room temperature observation of biexcitons in exfoliated WS2 monolayers. Applied Physics Letters, 2017, 110, .	3.3	54
116	Cell patterning via laser micro/nano structured silicon surfaces. Biofabrication, 2017, 9, 025024.	7.1	56
117	Ripple formation on silver after irradiation with radially polarised ultrashort-pulsed lasers. Journal of Applied Physics, 2017, 121, .	2.5	35
118	Short Pulse Laser Synthesis of Transition-Metal Dichalcogenide Nanostructures under Ambient Conditions. ACS Omega, 2017, 2, 2649-2656.	3.5	11
119	Biomimetic surface structuring using cylindrical vector femtosecond laser beams. Scientific Reports, 2017, 7, 45114.	3.3	137
120	Efficient and Highly Air Stable Planar Inverted Perovskite Solar Cells with Reduced Graphene Oxide Doped PCBM Electron Transporting Layer. Advanced Energy Materials, 2017, 7, 1602120.	19.5	188
121	Mimicking lizard-like surface structures upon ultrashort laser pulse irradiation of inorganic materials. Applied Surface Science, 2017, 418, 499-507.	6.1	56
122	Advanced Photonic Processes for Photovoltaic and Energy Storage Systems. Advanced Materials, 2017, 29, 1700335.	21.0	61
123	Ternary organic solar cells incorporating zinc phthalocyanine with improved performance exceeding 8.5%. Dyes and Pigments, 2017, 146, 408-413.	3.7	23
124	Ternary solution-processed organic solar cells incorporating 2D materials. 2D Materials, 2017, 4, 042005.	4.4	36
125	Partial ablation of Ti/Al nano-layer thin film by single femtosecond laser pulse. Journal of Applied Physics, 2017, 122, .	2.5	25
126	Improved Carrier Transport in Perovskite Solar Cells Probed by Femtosecond Transient Absorption Spectroscopy. ACS Applied Materials & amp; Interfaces, 2017, 9, 43910-43919.	8.0	90

#	Article	IF	CITATIONS
127	The role of chemical structure in indacenodithienothiophene- <i>alt</i> -benzothiadiazole copolymers for high performance organic solar cells with improved photo-stability through minimization of burn-in loss. Journal of Materials Chemistry A, 2017, 5, 25064-25076.	10.3	24
128	Low-temperature benchtop-synthesis of all-inorganic perovskite nanowires. Nanoscale, 2017, 9, 18202-18207.	5.6	65
129	Mimicking bug-like surface structures and their fluid transport produced by ultrashort laser pulse irradiation of steel. Applied Physics A: Materials Science and Processing, 2017, 123, 1.	2.3	62
130	Laser generated nanoparticles based photovoltaics. Journal of Colloid and Interface Science, 2017, 489, 28-37.	9.4	41
131	Biomimetic structures on steel via self-organization processes in multiple-scan, fs-laser irradiated surfaces. , 2017, , .		0
132	Ultrafast laser fabrication of biomimetic micro and nano structured surfaces with circular and vectorial polarization states. , 2017, , .		0
133	Spatial nonuniformity of excitonic properties in exfoliated WS <inf>2</inf> monolayers. , 2017, , .		0
134	Fabrication of Novel Biomimetic Structures on Steel Via Femtosecond Laser Over-Scans. , 2017, , .		0
135	Stainless steel surface wettability control via laser ablation in external electric field. Applied Physics A: Materials Science and Processing, 2016, 122, 1.	2.3	6
136	Structures for biomimetic, fluidic, and biological applications. MRS Bulletin, 2016, 41, 993-1001.	3.5	8
137	Photovoltaic Devices: Plasmonic Backscattering Effect in Highâ€Efficient Organic Photovoltaic Devices (Adv. Energy Mater. 2/2016). Advanced Energy Materials, 2016, 6, .	19.5	0
138	Graphene and transition metal dichalcogenide nanosheets as charge transport layers for solution processed solar cells. Materials Today, 2016, 19, 580-594.	14.2	79
139	Convection roll-driven generation of supra-wavelength periodic surface structures on dielectrics upon irradiation with femtosecond pulsed lasers. Physical Review B, 2016, 94, .	3.2	88
140	High steady-state column density of I(2P3/2) atoms from I2 photodissociation at 532 nm: Towards parity non-conservation measurements. Scientific Reports, 2016, 6, 33261.	3.3	1
141	Plasmonic Backscattering Effect in Highâ€Efficient Organic Photovoltaic Devices. Advanced Energy Materials, 2016, 6, 1501640.	19.5	43
142	Spatial non-uniformity in exfoliated WS <sub>2</sub> single layers. Nanoscale, 2016, 8, 16197-16203.	5.6	22
143	Solution processed reduced graphene oxide electrodes for organic photovoltaics. Nanoscale Horizons, 2016, 1, 375-382.	8.0	43
144	Highly efficient organic photovoltaic devices utilizing work-function tuned graphene oxide derivatives as the anode and cathode charge extraction layers. Journal of Materials Chemistry A, 2016, 4, 1612-1623.	10.3	74

#	Article	IF	CITATIONS
145	Electron field emission from graphene oxide wrinkles. RSC Advances, 2016, 6, 2768-2773.	3.6	29
146	Laser induced nucleation of plasmonic nanoparticles on two-dimensional nanosheets for organic photovoltaics. Journal of Materials Chemistry A, 2016, 4, 1020-1027.	10.3	47
147	Data in support on the shape of Schwann cells and sympathetic neurons onto microconically structured silicon surfaces. Data in Brief, 2015, 4, 636-640.	1.0	2
148	Microconical silicon structures influence NGFâ€induced PC12 cell morphology. Journal of Tissue Engineering and Regenerative Medicine, 2015, 9, 424-434.	2.7	35
149	From ripples to spikes: A hydrodynamical mechanism to interpret femtosecond laser-induced self-assembled structures. Physical Review B, 2015, 92, .	3.2	208
150	Gradient induced liquid motion on laser structured black Si surfaces. Applied Physics Letters, 2015, 107, .	3.3	43
151	Ternary Organic Solar Cells with Reduced Graphene Oxide–Sb <sub>2</sub> S <sub>3</sub> Hybrid Nanosheets as the Cascade Material. ChemNanoMat, 2015, 1, 346-352.	2.8	28
152	Effect of the reduction process on the field emission performance of reduced graphene oxide cathodes. RSC Advances, 2015, 5, 53604-53610.	3.6	11
153	Stability enhancement of organic photovoltaic devices utilizing partially reduced graphene oxide as the hole transport layer: nanoscale insight into structural/interfacial properties and aging effects. RSC Advances, 2015, 5, 106930-106940.	3.6	15
154	Ripple formation on nickel irradiated with radially polarized femtosecond beams. Optics Letters, 2015, 40, 5172.	3.3	67
155	Signatures of Quantized Energy States in Solutionâ€Processed Ultrathin Layers of Metalâ€Oxide Semiconductors and Their Devices. Advanced Functional Materials, 2015, 25, 1727-1736.	14.9	36
156	Reduced Graphene Oxide Micromesh Electrodes for Large Area, Flexible, Organic Photovoltaic Devices. Advanced Functional Materials, 2015, 25, 2213-2221.	14.9	118
157	Enhanced Stability of Aluminum Nanoparticle-Doped Organic Solar Cells. ACS Applied Materials & Interfaces, 2015, 7, 17756-17764.	8.0	41
158	Implantable vaccine development using in vitro antigen-pulsed macrophages absorbed on laser micro-structured Si scaffolds. Vaccine, 2015, 33, 3142-3149.	3.8	8
159	Laser fabricated discontinuous anisotropic microconical substrates as a new model scaffold to control the directionality of neuronal network outgrowth. Biomaterials, 2015, 67, 115-128.	11.4	80
160	Photovoltaics: Reduced Graphene Oxide Micromesh Electrodes for Large Area, Flexible, Organic Photovoltaic Devices (Adv. Funct. Mater. 15/2015). Advanced Functional Materials, 2015, 25, 2206-2206.	14.9	4
161	Functionalized Graphene as an Electron ascade Acceptor for Airâ€Processed Organic Ternary Solar Cells. Advanced Functional Materials, 2015, 25, 3870-3880.	14.9	67
162	Plasmonic Bulk Heterojunction Solar Cells: The Role of Nanoparticle Ligand Coating. ACS Photonics, 2015, 2, 714-723.	6.6	51

#	Article	IF	CITATIONS
163	Efficient ternary organic photovoltaics incorporating a graphene-based porphyrin molecule as a universal electron cascade material. Nanoscale, 2015, 7, 17827-17835.	5.6	42
164	Organic Solar Cells: Photochemical Synthesis of Solutionâ€Processable Graphene Derivatives with Tunable Bandgaps for Organic Solar Cells (Advanced Optical Materials 5/2015). Advanced Optical Materials, 2015, 3, 596-596.	7.3	1
165	High Electron Mobility Thinâ€Film Transistors Based on Solutionâ€Processed Semiconducting Metal Oxide Heterojunctions and Quasiâ€Superlattices. Advanced Science, 2015, 2, 1500058.	11.2	134
166	Programming the assembly of gold nanoparticles on graphene oxide sheets using DNA. Journal of Materials Chemistry C, 2015, 3, 9379-9384.	5.5	16
167	Efficiency enhancement of organic photovoltaic devices by embedding uncapped Al nanoparticles in the hole transport layer. RSC Advances, 2015, 5, 71704-71708.	3.6	17
168	Photochemical Synthesis of Solutionâ€Processable Graphene Derivatives with Tunable Bandgaps for Organic Solar Cells. Advanced Optical Materials, 2015, 3, 658-666.	7.3	41
169	Direct laser writing of flexible graphene field emitters. Applied Physics Letters, 2014, 105, .	3.3	38
170	High electron mobility thin-film transistors based on Ga2O3 grown by atmospheric ultrasonic spray pyrolysis at low temperatures. Applied Physics Letters, 2014, 105, .	3.3	56
171	Low and high repetition frequency femtosecond lasers processing of tungsten-based thin film. Laser and Particle Beams, 2014, 32, 613-619.	1.0	0
172	Laser-Assisted Reduction of Graphene Oxide for Flexible, Large-Area Optoelectronics. IEEE Journal of Selected Topics in Quantum Electronics, 2014, 20, 106-115.	2.9	59
173	Improving the efficiency of organic photovoltaics by tuning the work function of graphene oxide hole transporting layers. Nanoscale, 2014, 6, 6925-6931.	5.6	133
174	Enhanced Field Emission of WS <sub>2</sub> Nanotubes. Small, 2014, 10, 2398-2403.	10.0	45
175	Nanostructuring of single-crystal silicon carbide by femtosecond laser irradiation in a liquid. Physics of Wave Phenomena, 2014, 22, 15-18.	1.1	2
176	Laser-assisted nanostructuring of Silicon in liquid environment. Applied Physics A: Materials Science and Processing, 2014, 117, 359-364.	2.3	5
177	Enhanced Field Emission from Reduced Graphene Oxide Polymer Composites. ACS Applied Materials & Interfaces, 2014, 6, 388-393.	8.0	44
178	Controlled ultrashort-pulse laser-induced ripple formation on semiconductors. Applied Physics A: Materials Science and Processing, 2014, 114, 57-68.	2.3	40
179	Synergetic plasmonic effect of Al and Au nanoparticles for efficiency enhancement of air processed organic photovoltaic devices. Chemical Communications, 2014, 50, 5285-5287.	4.1	43
180	Intense femtosecond photoexcitation of bulk and monolayer MoS2. Applied Physics Letters, 2014, 105, .	3.3	52

#	Article	IF	CITATIONS
181	Synthesis of ultra-thin oxide layer in laser-treated 3×Â(Al/Fe)/Si multilayer structure. Journal of Materials Science, 2014, 49, 7900-7907.	3.7	1
182	The role of the ethynylene bond on the optical and electronic properties of diketopyrrolopyrrole copolymers. RSC Advances, 2014, 4, 58404-58411.	3.6	3
183	Elastic constants, viscosity and response time in nematic liquid crystals doped with ferroelectric nanoparticles. RSC Advances, 2014, 4, 46068-46074.	3.6	59
184	In situ photo-induced chemical doping of solution-processed graphene oxide for electronic applications. Journal of Materials Chemistry C, 2014, 2, 5931-5937.	5.5	26
185	Enhancement of the Efficiency and Stability of Organic Photovoltaic Devices via the Addition of a Lithium-Neutralized Graphene Oxide Electron-Transporting Layer. Chemistry of Materials, 2014, 26, 5988-5993.	6.7	71
186	Generation of nanoparticles of bronze and brass by laser ablation in liquid. Applied Surface Science, 2014, 302, 79-82.	6.1	26
187	Dispersion behaviour of graphene oxide and reduced graphene oxide. Journal of Colloid and Interface Science, 2014, 430, 108-112.	9.4	752
188	Aluminum nanoparticles for efficient and stable organic photovoltaics. RSC Advances, 2013, 3, 16288.	3.6	38
189	Post-fabrication, <i>in situ</i> laser reduction of graphene oxide devices. Applied Physics Letters, 2013, 102, .	3.3	76
190	Spatiallyâ€Resolved Inâ€Situ Structural Study of Organic Electronic Devices with Nanoscale Resolution: The Plasmonic Photovoltaic Case Study. Advanced Materials, 2013, 25, 4760-4765.	21.0	31
191	The influence of ultra-fast temporal energy regulation on the morphology of Si surfaces through femtosecond double pulse laser irradiation. Applied Physics A: Materials Science and Processing, 2013, 113, 273-283.	2.3	44
192	Effect of pulse duration on KrF laser treatment of a polyethersulfone film: cell culture study. Applied Physics A: Materials Science and Processing, 2013, 110, 633-637.	2.3	8
193	Nanoparticle-based plasmonic organic photovoltaic devices. Materials Today, 2013, 16, 133-146.	14.2	369
194	Flexible Organic Photovoltaic Cells with In Situ Nonthermal Photoreduction of Spin oated Graphene Oxide Electrodes. Advanced Functional Materials, 2013, 23, 2742-2749.	14.9	167
195	3-Dimensional Laser Structured Scaffolds Improve Macrophage Adherence and Antigen-specific Response. Procedia Engineering, 2013, 59, 211-218.	1.2	1
196	Plasmonic organic photovoltaic devices with graphene based buffer layers for stability and efficiency enhancement. Nanoscale, 2013, 5, 4144.	5.6	57
197	Organic solar cells with plasmonic layers formed by laser nanofabrication. Physical Chemistry Chemical Physics, 2013, 15, 8237.	2.8	42
198	Pulsed laser generation of novel nanomaterials for organic electronics. , 2013, , .		0

#	Article	IF	CITATIONS
199	Controlling ripples' periodicity using temporally delayed femtosecond laser double pulses. Optics Express, 2013, 21, 18501.	3.4	49
200	Femtosecond laser-induced periodic surface structure on the Ti-based nanolayered thin films. Journal of Applied Physics, 2013, 114, .	2.5	30
201	Direct laser texturing of biomimetic surfaces for neural tissue engineering. , 2013, , .		0
202	Laser-Based Biomimetic Tissue Engineering. Biological and Medical Physics Series, 2013, , 211-236.	0.4	3
203	Solution-processable graphene linked to 3,5-dinitrobenzoyl as an electron acceptor in organic bulk heterojunction photovoltaic devices. Carbon, 2012, 50, 5554-5561.	10.3	32
204	Enhancement of photo/thermal stability of organic bulk heterojunction photovoltaic devices via gold nanoparticles doping of the active layer. Nanoscale, 2012, 4, 7452.	5.6	70
205	Leaf surface characteristics and wetting in Ceratonia siliqua L Flora: Morphology, Distribution, Functional Ecology of Plants, 2012, 207, 551-556.	1.2	12
206	Tailoring the wetting properties of polymers from highly hydrophilic to superhydrophobic using UV laser pulses. Journal of Micromechanics and Microengineering, 2012, 22, 035001.	2.6	60
207	Dynamics of ripple formation on silicon surfaces by ultrashort laser pulses in subablation conditions. Physical Review B, 2012, 86, .	3.2	231
208	Organic Bulk Heterojunction Photovoltaic Devices Based on Polythiophene–Graphene Composites. ACS Applied Materials & Interfaces, 2012, 4, 4864-4870.	8.0	52
209	Porous nanoparticles of Al and Ti generated by laser ablation in liquids. Applied Surface Science, 2012, 258, 9283-9287.	6.1	40
210	Laser-assisted nanostructuring of Tungsten in liquid environment. Applied Surface Science, 2012, 258, 5898-5902.	6.1	27
211	Thermoplastic deformation of silicon surfaces induced by ultrashort pulsed lasers in submelting conditions. Journal of Applied Physics, 2012, 111, 053502.	2.5	44
212	Free-standing graphene on microstructured silicon vertices for enhanced field emission properties. Nanoscale, 2012, 4, 3069.	5.6	58
213	Properties of Silicon and Metal Oxide Electrowetting Systems. Journal of Adhesion Science and Technology, 2012, 26, 2143-2163.	2.6	8
214	Organic bulk heterojunction photovoltaic devices with surfactant-free Au nanoparticles embedded in the active layer. Applied Physics Letters, 2012, 100, .	3.3	94
215	Spin coated carbon nanotubes as the hole transport layer in organic photovoltaics. Solar Energy Materials and Solar Cells, 2012, 96, 298-301.	6.2	59
216	Nano-textured W shows improvement of thermionic emission properties. Applied Physics A: Materials Science and Processing, 2012, 106, 1-4.	2.3	32

#	Article	IF	CITATIONS
217	Nanomaterials by Ultrafast Laser Processing of Surfaces. Science of Advanced Materials, 2012, 4, 407-431.	0.7	63
218	KrF laser ablation of a polyethersulfone film: Effect of pulse duration on structure formation. Applied Surface Science, 2011, 258, 169-175.	6.1	17
219	Spin coated graphene films as the transparent electrode in organic photovoltaic devices. Thin Solid Films, 2011, 520, 1238-1241.	1.8	79
220	Plasmonic Organic Photovoltaic Devices on Transparent Carbon Nanotube Films. IEEE Transactions on Electron Devices, 2011, 58, 860-864.	3.0	28
221	Enhanced Structural Stability and Performance Durability of Bulk Heterojunction Photovoltaic Devices Incorporating Metallic Nanoparticles. Advanced Functional Materials, 2011, 21, 3573-3582.	14.9	105
222	Plasmonic organic photovoltaics doped with metal nanoparticles. Photonics and Nanostructures - Fundamentals and Applications, 2011, 9, 184-189.	2.0	40
223	Biomimetic micro/nanostructured functional surfaces for microfluidic and tissue engineering applications. Biomicrofluidics, 2011, 5, 13411.	2.4	168
224	Controlling cell adhesion via replication of laser micro/nano-textured surfaces on polymers. Biofabrication, 2011, 3, 045004.	7.1	50
225	Ultrafast laser micro/nano processing for microfluidic and tissue engineering apllications. , 2011, , .		1
226	Ultrafast electron dynamics in ZnO/Si micro-cones. Applied Physics A: Materials Science and Processing, 2010, 98, 701-705.	2.3	7
227	Tuning cell adhesion by controlling the roughness and wettability of 3D micro/nano silicon structures. Acta Biomaterialia, 2010, 6, 2711-2720.	8.3	395
228	From superhydrophobicity and water repellency to superhydrophilicity: smart polymer-functionalized surfaces. Chemical Communications, 2010, 46, 4136.	4.1	123
229	Electrowetting Properties of ZnO and TiO <sub>2</sub> Nanostructured Thin Films. Journal of Physical Chemistry C, 2010, 114, 10249-10253.	3.1	14
230	Electrowetting Properties of Micro/Nanostructured Black Silicon. Langmuir, 2010, 26, 13007-13014.	3.5	80
231	Generation of nanostructures on metals by laser ablation in liquids: new results. Quantum Electronics, 2010, 40, 1012-1020.	1.0	57
232	Silicon Scaffolds Promoting Three-Dimensional Neuronal Web of Cytoplasmic Processes. Tissue Engineering - Part C: Methods, 2010, 16, 497-502.	2.1	47
233	Three-dimensional carbon nanowall field emission arrays. Applied Physics Letters, 2010, 96, .	3.3	66
234	Laser structured biomimetic artificial surfaces that quantitatively reproduce the water repellency of		0

a Lotus leaf. , 2009, , .

#	Article	IF	CITATIONS
235	Photoinduced wettability transition and electrowetting in hierarchical ZnO and TiO <inf>2</inf> structures. , 2009, , .		0
236	Multifunctional and responsive surfaces based on fs laser micro/nano structuring of silicon. , 2009, ,		0
237	Laser-based micro/nanoengineering for biological applications. Progress in Quantum Electronics, 2009, 33, 127-163.	7.0	92
238	Femtosecond laser writing of nanostructures on bulk Al via its ablation in air and liquids. Applied Surface Science, 2009, 255, 5346-5350.	6.1	73
239	Reversible wettability of ZnO nanostructured thin films prepared by pulsed laser deposition. Thin Solid Films, 2009, 518, 1267-1270.	1.8	62
240	One pot direct hydrothermal growth of photoactive TiO2 films on glass. Journal of Photochemistry and Photobiology A: Chemistry, 2009, 202, 81-85.	3.9	27
241	Influence of solution chemistry on the properties of hydrothermally grown TiO2 for advanced applications. Catalysis Today, 2009, 144, 172-176.	4.4	28
242	Bio-inspired water repellent surfaces produced by ultrafast laser structuring of silicon. Applied Surface Science, 2009, 255, 5425-5429.	6.1	126
243	Generation of Al nanoparticles via ablation of bulk Al in liquids with short laser pulses. Optics Express, 2009, 17, 12650.	3.4	157
244	Laser writing of nanostructures on bulk Al via its ablation in liquids. Nanotechnology, 2009, 20, 105303.	2.6	78
245	Reversible Photoinduced Wettability Transition of Hierarchical ZnO Structures. Journal of Physical Chemistry C, 2009, 113, 2891-2895.	3.1	124
246	Polymer-nanotube composite mats with improved field emission performance and stability. Physical Chemistry Chemical Physics, 2009, 11, 703-709.	2.8	12
247	Surface nanotexturing of tantalum by laser ablation in water. Quantum Electronics, 2009, 39, 89-93.	1.0	50
248	Tailoring the wetting response of silicon surfaces via fs laser structuring. Applied Physics A: Materials Science and Processing, 2008, 93, 819.	2.3	93
249	Ultraviolet laser structuring of silicon carbide for cold cathode applications. Physica Status Solidi C: Current Topics in Solid State Physics, 2008, 5, 3309-3313.	0.8	5
250	Biomimetic Artificial Surfaces Quantitatively Reproduce the Water Repellency of a Lotus Leaf. Advanced Materials, 2008, 20, 4049-4054.	21.0	461
251	Light-induced reversible hydrophilicity of ZnO structures grown by aqueous chemical growth. Applied Surface Science, 2008, 254, 5695-5699.	6.1	67
252	Applications of ultrafast lasers in materials processing: fabrication on self-cleaning surfaces and scaffolds for tissue engineering. , 2008, , .		0

#	Article	IF	CITATIONS
253	Imaging Dielectric Properties of Si Nanowire Oxide with Conductive Atomic Force Microscopy Complemented with Femtosecond Laser Illumination. Nano Letters, 2008, 8, 1949-1953.	9.1	12
254	Part A: Bio-inspired water repellent surfaces produced by ultrafast laser structuring of silicon. , 2008, , .		0
255	Novel Aspects of Materials Processing by Ultrafast Lasers: From Electronic to Biological and Cultural Heritage Applications. Journal of Physics: Conference Series, 2007, 59, 266-272.	0.4	5
256	Integration of carbon nanotubes as hole transport electrode in polymer/fullerene bulk heterojunction solar cells. Thin Solid Films, 2007, 515, 8598-8600.	1.8	57
257	Silicon electron emitters fabricated by ultraviolet laser pulses. Applied Physics Letters, 2006, 88, 081103.	3.3	67
258	Atomic force microscopy based, multiphoton, photoelectron emission imaging. Applied Physics Letters, 2006, 89, 013110.	3.3	7
259	Making silicon hydrophobic: wettability control by two-lengthscale simultaneous patterning with femtosecond laser irradiation. Nanotechnology, 2006, 17, 3234-3238.	2.6	242
260	Metastable photoexpansion of hydrogenated amorphous silicon produced by exposure to short laser pulses. Journal of Non-Crystalline Solids, 2006, 352, 429-433.	3.1	0
261	Carbon nanotube/PEDOT:PSS electrodes for organic photovoltaics. EPJ Applied Physics, 2006, 36, 257-259.	0.7	56
262	Field-emission properties of arrays and extended areas of laser-fabricated silicon microstructures. Proceedings of the Institution of Mechanical Engineers, Part N: Journal of Nanoengineering and Nanosystems, 2006, 220, 143-150.	0.1	0
263	Photoinduced stress in hydrogenated amorphous silicon films. Applied Physics Letters, 2002, 80, 1734-1736.	3.3	24
264	Light induced stress in a-Si1â^'xGex:H alloys and its correlation with the Staebler–Wronski effect. Journal of Non-Crystalline Solids, 2002, 299-302, 521-524.	3.1	10
265	Elastic properties, intrinsic and photoinduced stress in hydrogenated amorphous-silicon thin films with different hydrogen content. Journal of Applied Physics, 2001, 89, 4294-4300.	2.5	29
266	Stress and internal friction associated with light-induced structural changes of a-Si:H deposited on crystalline silicon microcantilevers. Journal of Non-Crystalline Solids, 2000, 266-269, 506-510.	3.1	18
267	Space charges resulting from photocurrents exceeding the thermionic emission currents in a-Si:H. Journal of Non-Crystalline Solids, 2000, 266-269, 247-252.	3.1	1